



# Finite Difference Analysis of Unsteady MHD Free Convective Flow over Moving Semi-Infinite Vertical Cylinder with Chemical Reaction and Temperature Oscillation Effects

V. Rajesh<sup>1†</sup>, O. Anwar Bég<sup>2</sup> and Ch. Sridevi<sup>3</sup>

<sup>1</sup> *Department of Engineering Mathematics, GITAM University Hyderabad Campus, Rudraram, Patancheru Mandal, Medak Dist.-502 329, A.P. India.*

<sup>2</sup> *Gort Engovation (Aerospace Engineering Sciences), 15 Southmere Avenue, Bradford, BD7 3NU, England, UK.*

<sup>3</sup> *Department of Mathematics, Vidya Jyothi Institute of Technology, Aziz Nagar Gate, C.B. Post, Hyderabad-500075, A.P. India.*

†Corresponding Author Email: [v.rajesh.30@gmail.com](mailto:v.rajesh.30@gmail.com)

(Received August 19, 2014; accepted November 26, 2014)

## ABSTRACT

In the present study, the effects of chemical reaction on unsteady free convection flow of a viscous, electrically conducting, and incompressible fluid past a moving semi-infinite vertical cylinder with mass transfer and temperature oscillation is studied. The dimensionless governing partial differential equations are solved using an implicit finite-difference method of Crank–Nicolson type, which is stable and convergent. The transient velocity, transient temperature, and transient concentration profiles are studied for various parameters. The local as well as average skin-friction, Nusselt number, and Sherwood number are also analyzed and presented graphically. The results are compared with available computations in the literature, and are found to be in good agreement.

**Keywords:** Free convection; MHD; Implicit finite-difference method; Heat and mass transfer; First order chemical reaction; Temperature oscillation.

## NOMENCLATURE

$B_0$	magnetic field strength;	$U$	dimensionless velocity component in the $X$ -direction;
$C'$	species concentration of the fluid near the cylinder;	$V$	dimensionless velocity component in the $R$ -direction;
$C'_\infty$	concentration of the fluid at infinity;	$x$	spatial coordinate along the cylinder;
$C'_w$	concentration of the cylinder;	$X$	dimensionless spatial coordinate along the Cylinder
$C$	dimensionless species concentration;	$v$	velocity component in the $r$ -direction;
$D$	mass diffusion coefficient;	$\alpha$	thermal diffusivity;
$Gr$	thermal Grashof number;	$\beta$	volumetric thermal expansion coefficient;
$Gm$	mass Grashof number;	$\beta^*$	volumetric thermal expansion coefficient with concentration;
$g$	acceleration due to the gravity;	$\Delta t$	grid size in the time;
$Kr$	chemical reaction parameter;	$\Delta R$	grid size in the radial direction;
$M$	magnetic parameter;	$\Delta X$	grid size in the axial direction;
$\overline{Nu}$	average Nusselt number;	$\nu$	kinematic viscosity;
$Nux$	local Nusselt number;	$\rho$	density;
$Pr$	Prandtl number;		
$r$	spatial coordinate normal to the cylinder;		
$r_0$	radius of the cylinder;		
$R$	dimensionless spatial coordinate normal to		

	the cylinder;
$Sc$	Schmidt number;
$\overline{Sh}$	average Sherwood number;
$Sh$	local Sherwood number;
$T'$	temperature of the fluid near the cylinder;
$T'_\infty$	temperature of the fluid at infinity;
$T'_w$	temperature of the cylinder;
$T$	dimensionless temperature;
$t'$	time;
$t$	dimensionless time;
$u$	velocity component in the $x$ -direction;

$\sigma$	electrical conductivity of the fluid;
$\tau_x$	dimensionless local skin-friction;
$\bar{\tau}$	dimensionless average skin-friction;
$\omega'$	frequency of oscillation;
$\omega$	dimensionless frequency of oscillation.

#### Subscripts

$w$	conditions on the wall;
$\infty$	free stream condition;
$i$	grid point along the $X$ -direction;
$j$	grid point along the $R$ -direction.

#### Superscript

$k$	time step level.
-----	------------------

## 1. INTRODUCTION

Unsteady oscillatory free convective flows play an important role in chemical engineering, turbo-machinery, and aerospace technology. The rise of such flows is due to unsteady motion of either the boundary or the boundary temperature. Besides, the unsteadiness may also be due to the oscillatory free stream velocity or temperature. The phenomenon of heat and mass transfer is also very common in chemical process industries such as food processing and polymer production. Also the study of magneto hydrodynamics (MHD) incompressible viscous flows has many important engineering applications in devices such as MHD power generators, cooling of nuclear reactors, geothermal systems, aerodynamic processes, and heat exchange designs. Hossain (1988) solved the problem of simultaneous heat and mass transfer in two-dimensional (2D) free convection from a semi-infinite vertical plate. An integral method was used to find a solution for zero wall velocity with the small amplitude oscillatory wall temperature.

Several authors have studied the natural convection boundary layer flow of an electrically conducting fluid in the presence of a magnetic field. Emerly-Ashly (1963) presented the effect of a magnetic field upon the free convection of conducting fluids. An exact solution for the MHD flow between two rotating cylinders under a radial magnetic field was studied by Arora and Gupta (1972). Kumari and Nath (1999) studied the development of asymmetric flow of a viscous electrically conducting fluid in the forward stagnation point region of a 2D body and over a stretching surface with an applied magnetic field when the external stream or the stretching surface was set into impulsive motion from rest. The mass transfer effects on the flow past a vertical oscillating plate with variable temperature were given by Soundalgekar *et al.* (1994). It was observed that the skin friction increased with an increase in  $\omega t$ . Shankar and Krishan (1997) presented the effect of mass transfer on the MHD flow past an impulsively started infinite vertical plate. Soundalgekar *et al.* (1995) studied the effects of mass transfer on the flow past an oscillating infinite vertical plate with a constant heat flux. They showed that the skin friction for air

increased with the decrease in the molecular diffusivity of the species concentration when  $\omega t < \pi/4$ .

The situation, when the surface temperature on the vertical plate oscillates with the stream wise coordinate, has been investigated by many authors (Yang *et al.* (1982), Na (1978), Kao (1976), and Rees (1997)).

Rees (1997) studied, both numerically and analytically, the situation when the sinusoidal surface temperature oscillated about a constant mean value which was held above the ambient temperature of the fluid. Das *et al.* (1999) addressed the transient free convection flow past an infinite vertical plate with a periodic oscillation of the surface temperature. Li *et al.* (2001) investigated the steady and unsteady free convections from a vertical wall with stream-wise surface temperature oscillation. For small Grashof numbers, they obtained an asymptotic formula for the average Nusselt number by using a perturbation method. Zhang *et al.* (2004) numerically investigated the laminar natural convection on a periodically oscillating vertical flat plate heated at a uniform temperature, in which the temperature of the core fluid was assumed to vary in the vertical direction instead of the horizontal direction. Saeid (2004) investigated the periodic oscillation effect of the surface temperature on the transient free convection from a vertical plate, and showed that increasing the amplitude and frequency of the oscillating surface temperature could decrease the free convection heat transfer from the plate. Ganesan and Loganathan (2001) presented a numerical solution for the transient natural convection flow over a vertical cylinder under the combined buoyancy effect of heat and mass transfer by using an implicit finite difference scheme. Kishore *et al.* (2010) presented finite difference analysis of thermal radiation effects on the transient hydromagnetic natural convection flow past a vertical plate embedded in a porous medium with mass diffusion and fluctuating temperature about time at the plate, by taking into account the heat due to viscous dissipation. Loganathan *et al.* (2011) presented numerical solutions of magnetodynamics (MHD) effects on the free convective flow of an incompressible viscous fluid

past a moving semi-infinite vertical cylinder with temperature oscillation.

However, the present trend in the field of chemical reaction analysis is to give a mathematical model for the system to predict the reactor performance. A large amount of research has been reported in this field. In particular, the study of heat and mass transfer with chemical reaction is of considerable importance in chemical and hydrometallurgical industries. Chemical reaction can be codified as either heterogeneous or homogeneous processes. This depends on whether they occur at an interface or as a single phase volume reaction. A few representative fields of interest in which combined heat and mass transfer with chemical reaction effect play an important role are design of chemical processing equipment, formation and dispersion of fog, distribution of temperature and moisture over agricultural fields and groves of fruit trees, damage of crops due to freezing, food processing and cooling towers. For example, formation of smog is a first order homogeneous chemical reaction. Consider the emission of  $\text{NO}_2$  from automobiles and other smoke-stacks. This  $\text{NO}_2$  reacts chemically in the atmosphere with unburned hydrocarbons (aided by sunlight) and produces peroxyacetylnitrate, which forms an envelope of what is termed as 'photochemical smog'. All nature and most chemical fibers possess a shrinking potential, i.e., as soon as they with water and/or warmth come into contact, they change their form and run in. The order of the chemical reaction depends on several factors. The simplest chemical reaction is the first order reaction in which the rate of reaction is directly proportional to the species concentration.

Chambre and Young (1958) have analyzed a first order chemical reaction in the neighbourhood of a horizontal plate. Dass *et al.* (1994) have studied the effect of homogeneous first order chemical reaction on the flow past an impulsively started infinite vertical plate with uniform heat flux and mass transfer. Again, mass transfer effects on moving isothermal vertical plate in the presence of chemical reaction was studied by Dass *et al.* (1999). The dimensionless governing equations were solved by the usual Laplace Transform technique. Muthucumaraswamy and Ganesan (2000) studied the problem of an impulsive motion of a vertical plate with heat flux and diffusion of chemically reactive species. Chamkha and Ahmed (2011) analyzed unsteady mixed convection heat and mass transfer near the stagnation point of a three-dimensional porous body in the presence of magnetic field, chemical reaction and heat source or sink. Bisht *et al.* (2011) investigated the steady incompressible mixed convection boundary layer flow with variable fluid properties and mass transfer inside a cone due to a point sink at the vertex of the cone. Uddin *et al.* (2011) studied the distribution of the chemically reactant solute in the MHD flow of an electrically conducting viscous incompressible fluid over a stretching surface.

Rajesh (2012) studied the effects of mass transfer on flow past an impulsively started infinite vertical plate with Newtonian heating and chemical reaction. Rajesh *et al.* (2013) numerically studied radiation and chemical reaction effects on unsteady MHD free convection flow of a dissipative fluid past an infinite vertical plate with Newtonian heating. Recently Choudhury and Das (2014) studied visco-elastic free convective transient MHD flow over a vertical porous plate through porous media in presence of radiation and chemical reaction with heat and mass transfer.

The present study considers the chemical reaction effects on the transient MHD free convective flow of an incompressible viscous electrically conducting fluid past a semi-infinite moving vertical cylinder with temperature oscillation. The governing boundary layer equations along with the initial and boundary conditions are first cast into a dimensionless form, and the resulting equations are then solved by an implicit finite difference method of the Crank-Nicolson type.

## 2. MATHEMATICAL THERMO FLUID DYNAMIC MODEL

An unsteady, laminar, two-dimensional, combined heat and mass transfer boundary layer flow of a viscous incompressible fluid past a semi-infinite moving vertical cylinder of radius  $r_0$  is considered.

The  $x$ -axis is taken along the axis of the cylinder in the vertically upward direction, and the radial coordinate  $r$  is taken along the direction of the magnetic field.  $x$  and  $r$  are mutually perpendicular as shown in Figure 1. The gravitational acceleration  $g$  is acting downward. Initially, both the cylinder and the fluid are stationary at the same temperature  $T'_\infty$  and the same concentration level  $C'_\infty$ . They are maintained at the same level for all  $t' \leq 0$ . At time  $t' > 0$ , the cylinder starts moving in the vertical direction with a uniform velocity  $u_0$ . The temperature on the surface of the cylinder is raised to  $T'_w$  and a periodic temperature is assumed to be superimposed on this mean constant temperature of the surface. Also, the concentration on the surface of the cylinder is raised to  $C'_w$ . All the fluid properties are assumed to be constant except the influence of the density variation, which induces the buoyancy force. The effect of viscous dissipation is not considered in the energy equation.

There exists a homogeneous first order chemical reaction between the fluid and species concentration. The system is considered to be axis symmetric. The induced current does not distort the magnetic field. The magnetic field is constant in a direction perpendicular to the cylinder. The coefficient of electrical conductivity is constant and scalar throughout the fluid.

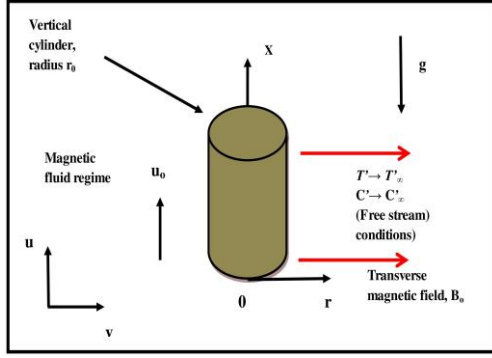


**Fig. 1. The physical model and coordinate system.**

Under the above assumptions and taking the usual Boussinesq approximation into account, the governing equations for continuity, momentum, energy, and concentration are as follows:

$$\frac{\partial(ru)}{\partial x} + \frac{\partial(rv)}{\partial r} = 0 \quad (1)$$

$$\frac{\partial u}{\partial t'} + u \frac{\partial u}{\partial x} + v \frac{\partial u}{\partial r} = g\beta(T' - T'_\infty) + g\beta^*(C' - C'_\infty) + \frac{v}{r} \frac{\partial}{\partial r} \left( r \frac{\partial u}{\partial r} \right) - \frac{\sigma B_0^2}{\rho} u \quad (2)$$

$$\frac{\partial T'}{\partial t'} + u \frac{\partial T'}{\partial x} + v \frac{\partial T'}{\partial r} = \frac{\alpha}{r} \frac{\partial}{\partial r} \left( r \frac{\partial T'}{\partial r} \right) \quad (3)$$

$$\frac{\partial C'}{\partial t'} + u \frac{\partial C'}{\partial x} + v \frac{\partial C'}{\partial r} = \frac{D}{r} \frac{\partial}{\partial r} \left( r \frac{\partial C'}{\partial r} \right) - K_r'(C' - C'_\infty) \quad (4)$$

Equations (1)–(4) are subjected to the following initial and boundary conditions:

$$\begin{aligned} t' \leq 0: & u = 0, v = 0, T' = T'_\infty, C' = C'_\infty \\ & \text{for all } x \geq 0 \text{ and } r \geq 0 \\ t' > 0: & u = u_0, v = 0, C' = C'_w, \\ & T' = T'_w + (T'_w - T'_\infty) \cos(\omega t') \text{ at } r = r_0 \\ & u = 0, T' = T'_\infty, C' = C'_\infty \text{ at } x = 0 \text{ and } r \geq r_0 \\ & u' \rightarrow 0, T' \rightarrow T'_\infty, C' \rightarrow C'_\infty \text{ as } r \rightarrow \infty \end{aligned} \quad (5)$$

Introduce the following non-dimensional variables and parameters:

$$\begin{aligned} X &= \frac{xv}{u_0 r_0^2}, R = \frac{r}{r_0}, U = \frac{u}{u_0}, V = \frac{vr_0}{v}, t = \frac{t'v}{r_0^2}, \\ T &= \frac{T' - T'_\infty}{T'_w - T'_\infty}, \text{Pr} = \frac{v}{\alpha}, M = \frac{\sigma B_0^2 r_0^2}{\rho v}, \\ K_r &= \frac{K_r' r_0^2}{v}, \omega = \frac{r_0^2 \omega'}{v}, C = \frac{C' - C'_\infty}{C'_w - C'_\infty}, Sc = \frac{v}{D}, \\ Gr &= \frac{g\beta r_0^2 (T'_w - T'_\infty)}{u_0 v}, Gm = \frac{g\beta^* r_0^2 (C'_w - C'_\infty)}{u_0 v} \end{aligned} \quad (6)$$

Then, Equations (1) – (4) can be reduced to the following forms:

$$\frac{\partial(RU)}{\partial X} + \frac{\partial(RV)}{\partial R} = 0 \quad (7)$$

$$\begin{aligned} \frac{\partial U}{\partial t} + U \frac{\partial U}{\partial X} + V \frac{\partial U}{\partial R} \\ = GrT + GmC + \frac{1}{R} \frac{\partial}{\partial R} \left( R \frac{\partial U}{\partial R} \right) - MU \end{aligned} \quad (8)$$

$$\frac{\partial T}{\partial t} + U \frac{\partial T}{\partial X} + V \frac{\partial T}{\partial R} = \frac{1}{\text{Pr}} \frac{1}{R} \frac{\partial}{\partial R} \left( R \frac{\partial T}{\partial R} \right) \quad (9)$$

$$\begin{aligned} \frac{\partial C}{\partial t} + U \frac{\partial C}{\partial X} + V \frac{\partial C}{\partial R} \\ = \frac{1}{\text{Sc}} \frac{1}{R} \frac{\partial}{\partial R} \left( R \frac{\partial C}{\partial R} \right) - K_r C \end{aligned} \quad (10)$$

The corresponding initial and boundary conditions in non-dimensional quantities are given by

$$\begin{aligned} t \leq 0: & U = 0, V = 0, T = 0, C = 0 \\ & \text{for all } X \text{ and } R \\ t > 0: & U = 1, V = 0, T = 1 + \cos(\omega t), \\ & C = 1 \text{ at } R = 1 \\ & U = 0, T = 0, C = 0 \text{ at } X = 0 \\ & U \rightarrow 0, T \rightarrow 0, C \rightarrow 0 \text{ as } R \rightarrow \infty \end{aligned} \quad (11)$$

### 3. NUMERICAL TECHNIQUE

In order to solve these unsteady, non-linear coupled equations (7) to (10) under the boundary conditions (11), an implicit finite difference method of Crank–Nicolson type has been employed. The finite difference equations corresponding to Eqns. (7) – (10) are as follows:

$$\begin{aligned} & \left[ \frac{U_{i,j}^{n+1} - U_{i-1,j}^{n+1} + U_{i,j}^n - U_{i-1,j}^n}{4\Delta X} \right. \\ & \left. + \frac{V_{i,j}^{n+1} - V_{i,j-1}^{n+1} + V_{i,j}^n - V_{i,j-1}^n}{2\Delta R} \right. \\ & \left. + \frac{V_{i,j}^{n+1}}{1 + (j-1)\Delta R} \right] = 0 \quad (12) \\ & \left[ \frac{U_{i,j}^{n+1} - U_{i,j}^n}{\Delta t} \right. \\ & \left. + U_{i,j}^n \left[ \frac{U_{i,j}^{n+1} - U_{i-1,j}^{n+1} + U_{i,j}^n - U_{i-1,j}^n}{2\Delta X} \right] \right. \\ & \left. + V_{i,j}^n \left[ \frac{U_{i,j+1}^{n+1} - U_{i,j-1}^{n+1} + U_{i,j+1}^n - U_{i,j-1}^n}{4\Delta R} \right] \right. \\ & = \frac{Gr}{2} [T_{i,j}^{n+1} + T_{i,j}^n] + \frac{Gm}{2} [C_{i,j}^{n+1} + C_{i,j}^n] \\ & \left. + \frac{U_{i,j-1}^{n+1} - 2U_{i,j}^{n+1} + U_{i,j+1}^{n+1}}{2(\Delta R)^2} \right. \\ & \left. + \frac{U_{i,j-1}^n - 2U_{i,j}^n + U_{i,j+1}^n}{2(\Delta R)^2} \right. \\ & \left. + \frac{U_{i,j+1}^{n+1} - U_{i,j-1}^{n+1} + U_{i,j+1}^n - U_{i,j-1}^n}{4[1 + (j-1)\Delta R]\Delta R} \right] \end{aligned}$$

$$-M \left[ \frac{U_{i,j}^{n+1} + U_{i,j}^n}{2} \right] \quad (13)$$

$$\begin{aligned} & \left[ \frac{T_{i,j}^{n+1} - T_{i,j}^n}{\Delta t} \right] \\ & + U_{i,j}^n \left[ \frac{T_{i,j}^{n+1} - T_{i-1,j}^{n+1} + T_{i,j}^n - T_{i-1,j}^n}{2\Delta X} \right] \\ & + V_{i,j}^n \left[ \frac{T_{i,j+1}^{n+1} - T_{i,j-1}^{n+1} + T_{i,j+1}^n - T_{i,j-1}^n}{4\Delta R} \right] \\ & = \left[ \frac{T_{i,j-1}^{n+1} - 2T_{i,j}^{n+1} + T_{i,j+1}^{n+1} + T_{i,j-1}^n - 2T_{i,j}^n + T_{i,j+1}^n}{2Pr(\Delta R)^2} \right] \\ & + \left[ \frac{T_{i,j+1}^{n+1} - T_{i,j-1}^{n+1} + T_{i,j+1}^n - T_{i,j-1}^n}{4Pr[1+(j-1)\Delta R] \Delta R} \right] \end{aligned} \quad (14)$$

$$\begin{aligned} & \left[ \frac{C_{i,j}^{n+1} - C_{i,j}^n}{\Delta t} \right] \\ & + U_{i,j}^n \left[ \frac{C_{i,j}^{n+1} - C_{i-1,j}^{n+1} + C_{i,j}^n - C_{i-1,j}^n}{2\Delta X} \right] \\ & + V_{i,j}^n \left[ \frac{C_{i,j+1}^{n+1} - C_{i,j-1}^{n+1} + C_{i,j+1}^n - C_{i,j-1}^n}{4\Delta R} \right] \\ & = \left[ \frac{C_{i,j-1}^{n+1} - 2C_{i,j}^{n+1} + C_{i,j+1}^{n+1} + C_{i,j-1}^n - 2C_{i,j}^n + C_{i,j+1}^n}{2Sc(\Delta R)^2} \right] \\ & + \left[ \frac{C_{i,j+1}^{n+1} - C_{i,j-1}^{n+1} + C_{i,j+1}^n - C_{i,j-1}^n}{4Sc[1+(j-1)\Delta R] \Delta R} \right] \\ & - Kr \left[ \frac{C_{i,j}^{n+1} + C_{i,j}^n}{2} \right] \end{aligned} \quad (15)$$

The region of integration is considered as a rectangle with sides  $X_{max} = 1.0$  and  $R_{max} = 20.0$ , where  $R_{max}$  corresponds to  $R \rightarrow \infty$  which lies very well outside the momentum, thermal and concentration boundary layers. Here, the subscript  $i$  - designates the grid point along the X-direction,  $j$  - along the R-direction and the superscript  $n$  along the t-direction. During any one-time step, coefficients  $U_{i,j}^n$  and  $V_{i,j}^n$  appearing in the difference equations are treated as constants. The values of U, V, T and C are known at all grid points at  $t = 0$  from the initial conditions. The computations of U, V, T and C at time level (n+1)

using the known values at previous time level (n) are calculated as follows: The finite difference equation (15) at every internal nodal point on a particular  $i$ -level, constitute a tri-diagonal system of equations. Such a system of equations is solved by Thomas algorithm as described in Carnahan *et al.* (1969). Thus, the values of C are found at every nodal point on a particular  $i$  at (n+1)<sup>th</sup> time level. Similarly the values of T are calculated from Eq. (14). Using the values of C and T at (n+1)<sup>th</sup> time level in Eq. (13), the values of U at (n+1)<sup>th</sup> time level are found in a similar manner. Thus the values of C, T and U are known on a particular  $i$ -level. The values of V are calculated explicitly using Eq. (12) at every nodal point on a particular  $i$ -level at (n+1)<sup>th</sup> time level. This process is repeated for various  $i$ -levels. Thus the values of C, T, U and V are known at all grid points in the rectangular region at (n+1)<sup>th</sup> time level. After experimenting with a few sets of mesh sizes, the mesh sizes are fixed at the level  $\Delta X = 0.02$  and  $\Delta R = 0.2$  with the time step  $\Delta t = 0.02$ . In this case, the spatial mesh sizes are reduced by 50% in one direction. Then, the results in both directions X and R are compared. It is observed that, when the mesh size is reduced by 50% in the R-direction, the results differ in the fifth place after the decimal point; while when the mesh sizes are reduced by 50% in the X-direction or in both directions X and R, the results are correct to the fourth decimal place. Therefore, these mesh sizes are considered to be appropriate for calculations. The finite difference scheme is unconditionally stable as discussed in Ganesan and Rani (1998). The truncation error in the finite-difference approximation is  $O(\Delta t^2 + \Delta R^2 + \Delta X)$  and it tends to zero as  $\Delta t$ ,  $\Delta R$ , and  $\Delta X$  tend to zero. Therefore, the scheme is compatible. The stability and the compatibility ensure the convergence.

#### 4. RESULTS AND DISCUSSION

During the initial period, the body forces have not had sufficient time to generate any appreciable motion in the fluid. Hence, both velocity components are negligible for small time  $t$ . During this initial transient regime, the heat transfer process is dominated by pure heat conduction. The temperature distribution at early times is, therefore, the same as the transient conduction problem in a semi-infinite solid. The temperature distribution in a semi-infinite solid is given by the following equation (Schlichting (1979) and Carslaw and Jaeger (1959)),

$$T' = \left( \frac{r_0}{r} \right)^{1/2} \operatorname{erfc} \left( \frac{r - r_0}{2\sqrt{\alpha t'}} \right) \quad (16)$$

with the initial and boundary conditions:

$$t' \leq 0 : T' = T'_\infty \text{ for all } r$$

$$t' > 0 : T' = T'_w \text{ at } r = r_0$$

By introducing the non-dimensional quantities defined in Eq. (6), the transient temperature distribution in a semi-infinite solid can be written as

$$T = R^{-1/2} \operatorname{erfc} \left( \frac{R-1}{2\sqrt{t/\operatorname{Pr}}} \right) \quad (17)$$

with the initial and boundary conditions:

$$t \leq 0: T = 0 \text{ for all } R$$

$$t > 0: T = 1 \text{ at } R = 1$$

Figure 2 shows the comparison between the transient temperature distribution calculated by Eq. (17) and by the current finite difference method (when  $\omega t = \pi/2$ ) at two different early times. They are found to be in excellent agreement and this shows that the current finite difference method is valid for this type of transient problem.

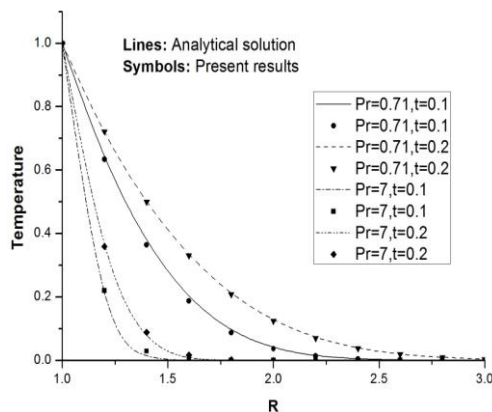


Fig. 2. Comparison of temperature profiles.

In order to study the behaviour of velocity  $u$ , temperature  $T$  and concentration  $C$  fields, a comprehensive numerical computation is carried out for various values of the parameters that describe the flow characteristics and the results are reported in terms of graphs. To be more realistic, all the computations are carried out for  $Pr = 0.71$  (i.e., for air), 7 (i.e., for water) and the corresponding values of  $Sc$  are chosen such that they represent water vapour (0.6), carbon dioxide (0.94) at temperature  $25^\circ\text{C}$  and 1 atmospheric pressure. Grashof number ( $Gr$ ) for heat transfer is chosen to be  $Gr = 2, 5$ , and the solutal Grashof number ( $Gm$ ) for mass transfer  $Gm = 2, 5$ , which corresponds to the case of cooling of the surface. Magnetic field parameter  $M = 2, 5$ , Chemical reaction parameter  $K = 2, 5$  and phase angle  $\omega t = \pi/2, \pi/3$ .

The transient velocity profiles for various values of Magnetic field parameter  $M$ , Chemical reaction parameter  $Kr$  and phase angle  $\omega t$  are presented in Fig. 3. It is observed from Fig. 3 that as the magnetic parameter  $M$  increases, the flow rate retards and thereby results in to a decrease in the velocity profiles. Thus momentum boundary layer thickness decreases with increasing values of  $M$ . The reason behind this phenomenon is that application of magnetic field to an electrically conducting fluid gives rises to a resistive type force called the Lorentz force. This force has the tendency to slow down the motion of the fluid in the boundary layer. It is also observed from Fig. 3 that fluid velocity  $u$  decreases on increasing Chemical reaction parameter in the boundary layer

region. This implies that Chemical reaction parameter decelerates fluid velocity. It is found that an increase in the phase angle  $\omega t$  leads to a fall in the fluid velocity. It is also noticed from Fig. 3 that fluid velocity is maximum in the vicinity of the cylinder surface and then decreases properly on increasing boundary layer coordinate  $R$  to approach the free stream value for all  $M, Kr$  and  $\omega t$ .

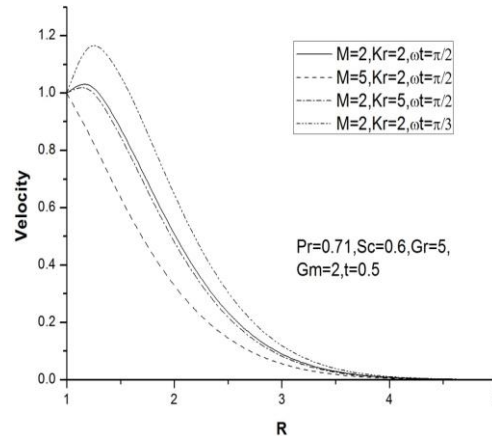


Fig. 3. Transient velocity profiles at  $X=1.0$  for different  $M, Kr, \omega t$ .

The transient velocity profiles for various values of thermal Grashof number  $Gr$ , mass Grashof number  $Gm$  and Schmidt number  $Sc$  are presented in Fig. 4. Since Grashof number  $Gr$  signifies the relative effects of thermal buoyancy force to viscous hydrodynamic force in the boundary layer region, it is observed from Fig. 4 that an increase in  $Gr$  leads to an increase in fluid velocity in the boundary layer region. This implies that thermal buoyancy force tends to accelerate fluid flow. It is also observed that the velocity of fluid increases with increase in  $Gm$ . It is due to the fact that increase in the values of mass Grashof number has the tendency to increase the mass buoyancy effect. This gives rise to an increase in the induced flow. It is also observed from Fig. 4 that the velocity decreases with increasing Schmidt number in the boundary layer region. An increasing Schmidt number implies that viscous forces dominate over the diffusion effects. Schmidt number in free convection flow regimes, in fact, represents the relative effectiveness of momentum and mass transport by diffusion in the velocity (momentum) and concentration (species) boundary layers. Therefore an increase in  $Sc$  will counter-act momentum diffusion since viscosity effects will increase and molecular diffusivity will be reduced. The flow will therefore be decelerated with a rise in  $Sc$ .

Figure 5 reveals the effects of  $t$  and  $Pr$  on the transient velocity profiles. It is evident from the figure that the velocity increases with an increase in time for both air and water. Furthermore, the velocity attains its maximum value in the vicinity of the cylinder and then fades away. The magnitude of velocity for  $Pr = 0.71$  is much higher than that of  $Pr = 7$ . Physically, this is possible because fluids with high Prandtl numbers have high viscosity and hence move slowly.

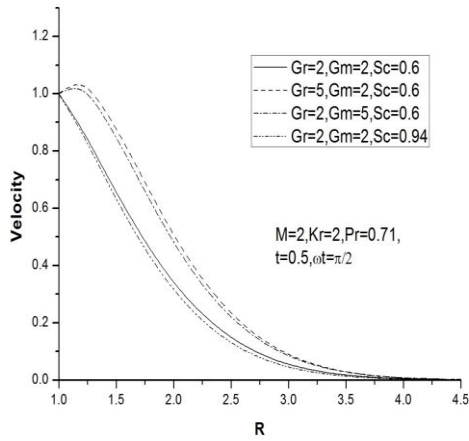


Fig. 4. Transient velocity profiles at X=1.0 for different Gr, Gm, Sc.

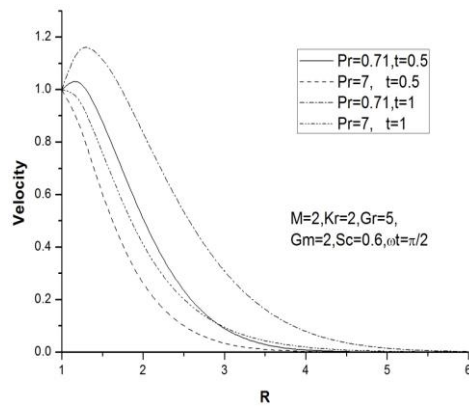


Fig. 5. Transient velocity profiles at X=1.0 for different Pr, t.

Figure 6 displays the transient temperature profiles against R for different Pr,  $\omega t$  and t. The magnitude of temperature is maximum at the cylinder and then decays to zero asymptotically. The temperature falls owing to an increase in the value of  $\omega t$  for air (Pr = 0.71). The magnitude of temperature for air (Pr = 0.71) is greater than that for water (Pr = 7); this is due to the fact that the thermal conductivity of fluid decreases with increasing Pr, resulting in a decrease in thermal boundary layer thickness. It is also evident from the figure that the temperature increases with an increase in time for air (Pr = 0.71).

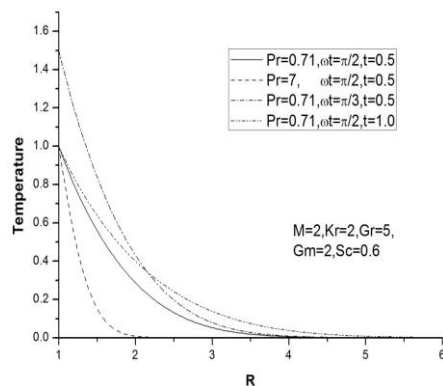


Fig. 6. Transient temperature profiles at X=1.0 for different Pr,  $\omega t$ , t.

The Concentration profiles for different values of Kr, Sc,  $\omega t$  and time t and are presented in Fig.7. It is noticed from Fig. 7 that the fluid concentration is maximum at the surface of the cylinder and it decreases on increasing boundary layer coordinate R to approach free stream value. It is observed from Fig. 7 that fluid concentration C decreases on increasing chemical reaction parameter Kr or Schmidt number Sc in the boundary layer region which implies that chemical reaction or Schmidt number tends to reduce fluid concentration. It is also noticed from Fig. 7 that fluid concentration C increases on increasing time t in the boundary layer region which implies that there is an enhancement in fluid concentration as time progresses. Also, it is found that the effect of  $\omega t$  on concentration is negligible.

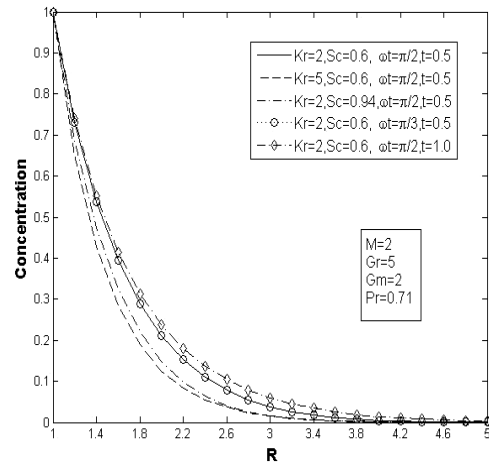


Fig. 7. Transient concentration profiles at X=1.0 for different Kr, Sc,  $\omega t$ , t.

Knowing the velocity, temperature and concentration profiles, it is important to study the local and average skin-friction, the rate of heat transfer and mass transfer. The local as well as average skin-friction, Nusselt number, and Sherwood number in terms of dimensionless quantities are given by

$$\tau_x = -\left(\frac{\partial U}{\partial R}\right)_{R=1} \quad (18)$$

$$\bar{\tau} = -\int_0^1 \left(\frac{\partial U}{\partial R}\right)_{R=1} dX \quad (19)$$

$$Nu_x = -X \left(\frac{\partial T}{\partial R}\right)_{R=1} \quad (20)$$

$$\bar{Nu} = -\int_0^1 \left(\frac{\partial T}{\partial R}\right)_{R=1} dX \quad (21)$$

$$Sh_x = -X \left(\frac{\partial C}{\partial R}\right)_{R=1} \quad (22)$$

$$\bar{Sh} = -\int_0^1 \left(\frac{\partial C}{\partial R}\right)_{R=1} dX \quad (23)$$

The derivatives involved in Eqs. (18)– (23) are evaluated by using a *five-point approximation formula*. Then, the integrals are evaluated by using the *Newton-Cotes formula*.

Figs. 8 - 13 present the local and average values of skin friction for different  $M$ ,  $Kr$ ,  $\omega t$ ,  $Gr$ ,  $Gm$ ,  $Sc$  and  $Pr$  values. It is observed from the Figs. 8-13, that the rise in  $M$ ,  $Kr$ ,  $Sc$ ,  $Pr$ ,  $\omega t$  increase the local and average values of the skin friction while an opposite effect is observed for  $Gr$  and  $Gm$ . It is also observed that the local skin friction is decreasing with increasing  $x$  or  $t$  values. But this decrease in local skin friction with  $t$  is negligible up to certain  $x$  value from  $x=0$ . Also the average skin friction is found to decrease exponentially with increasing time for all  $M$ ,  $Kr$ ,  $\omega t$ ,  $Gr$ ,  $Gm$ ,  $Sc$  and  $Pr$  values.

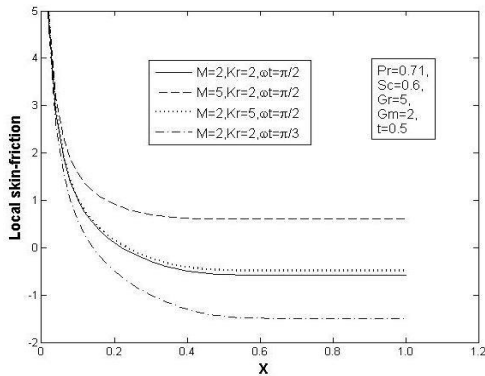


**Fig. 8.** Local skin-friction for different  $M$ ,  $Kr$ ,  $\omega t$ .

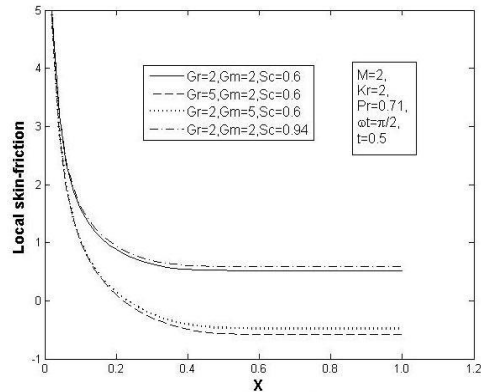


**Fig. 9.** Local skin-friction for different  $Gr$ ,  $Gm$ ,  $Sc$ .

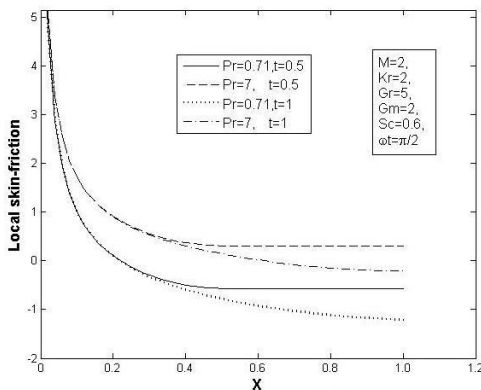


**Fig. 10.** Local skin-friction for different  $Pr$ ,  $t$ .

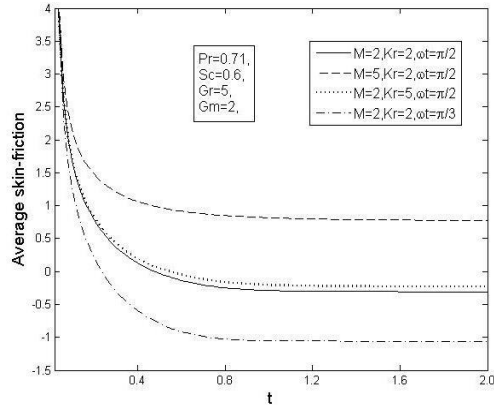


**Fig. 11.** Average skin-friction for different  $M$ ,  $Kr$ ,  $\omega t$ .

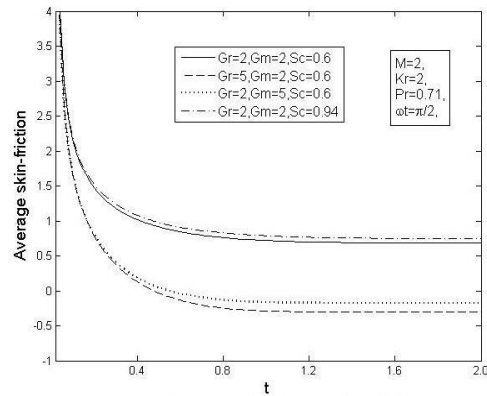


**Fig. 12.** Average skin-friction for different  $Gr$ ,  $Gm$ ,  $Sc$ .

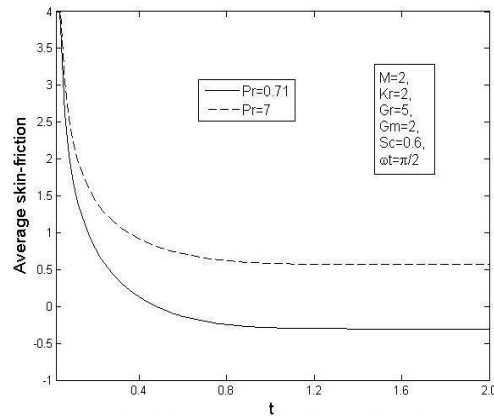


**Fig. 13.** Average skin-friction for different  $Pr$ ,  $\omega t$ .

Figs. 14 - 15 show the distributions of local and average values of Nusselt number with different  $Pr$  and  $\omega t$  values. Both local and average Nusselt number increase with the increasing values of  $Pr$ . Since an increase in  $Pr$  decreases the temperature profiles this will manifest with an escalation in the wall temperature gradient i.e. greater heat will be conveyed from the fluid to the wall. Heat transfer rates to the wall will therefore be elevated manifesting in a boost in Nusselt number. But the local and average values of Nusselt number decrease with the increasing values of  $\omega t$ .

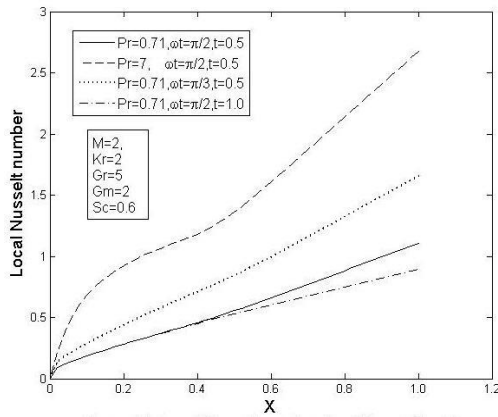


**Fig. 14. Local Nusselt number for different  $Pr, \omega t, t$ .**

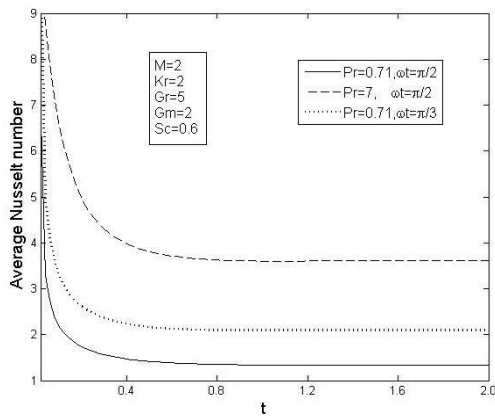


**Fig. 15. Average Nusselt number for different  $Pr$ ,**

It is also noticed that local Nusselt number increases with increasing  $x$  and decreases with increasing time  $t$ . But this decrease in local Nusselt number is negligible up to certain  $x$  value from  $x=0$ . The average Nusselt number is found high initially and then it starts decreasing with increasing time up to certain value and then it remains constant.

Finally Figs. 16-17 show the variation of local and average Sherwood number with different  $Kr, Sc$  and  $\omega t$  values. Consistently there is an ascent in both local and average Sherwood number with a rise in Schmidt number or chemical reaction parameter. Increasing Schmidt number or chemical reaction parameter depresses the concentration profiles and this implies greater diffusion of species to the wall i.e. an increase in concentration gradients at the wall. This rise in the concentration gradient increases the mass transfer, and hence increases the Sherwood number. It is also noticed that the increases in phase angle  $\omega t$  decrease the average values of the Sherwood number while this effect is negligible on the local Sherwood number. It is also clear from Figures that the local Sherwood number increases with increasing  $x$ , and decreases with increasing time. Lastly, the average Sherwood number is found to decrease with increasing time up to certain value and after that it remains constant.

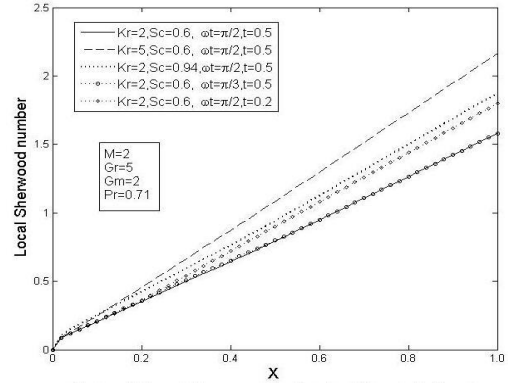


**Fig. 16. Local Sherwood number for different  $Kr, Sc, t, \omega t$ .**

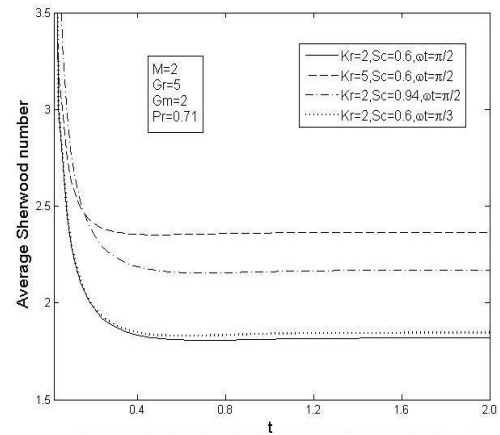


**Fig. 17. Average Sherwood number for different  $Kr, Sc, \omega t$ .**

## 5. CONCLUSIONS

A detailed numerical study has been carried out for the effects of chemical reaction of first order on the transient magneto hydrodynamics (MHD) free convective flow of an incompressible viscous electrically conducting fluid past a moving semi-infinite vertical cylinder with temperature oscillation. A family of governing partial differential equations is solved by an implicit finite difference scheme of Crank–Nicolson type, which is stable and convergent. The results are obtained for different values of chemical reaction parameter  $Kr$ , magnetic field parameter  $M$ , phase angle  $\omega t$ , thermal Grashof number  $Gr$ , mass Grashof number  $Gm$ , Schmidt number  $Sc$  and prandtl number  $Pr$ . Conclusions of this study are as follows.

1. Velocity increases with the increasing  $Gr, Gm$  and decreases with the increasing values of  $Kr, M, Sc, Pr$  and  $\omega t$ .
2. Temperature decreases with the increasing  $Pr$  and  $\omega t$ .
3. Concentration decreases with the increasing  $Kr$  and  $Sc$ .
4. Local and average skin friction increase with increasing  $M, Kr, Sc, Pr$  and  $\omega t$ .
5. Local and average skin friction decrease with increasing  $Gr$  and  $Gm$ .
6. Local and average Nusselt number increase

- with the increasing values of  $Pr$ .
7. Local and average Nusselt number decrease with the increasing values of  $\omega t$ .
  8. Local and average values of Sherwood number increases with increasing  $Kr$  and  $Sc$ .
  9. An increase in phase angle  $\omega t$  decreases the average Sherwood number, while this effect is negligible on the local Sherwood number.

#### ACKNOWLEDGEMENTS

The authors are grateful to the Editor and Reviewers of this journal, for their constructive comments which have helped to improve the present article.

#### REFERENCES

- Arora, K. L. and P. R. Gupta (1972). Magneto-hydrodynamic flows between two rotating coaxial cylinders under radial magnetic field. *Physics of Fluids* 15(6), 1146-1147.
- Bisht, V., M. Kumar and Z. Uddin (2011). Effects of Variable Thermal Conductivity and Chemical Reaction on Steady Mixed Convection Boundary Layer Flow with Heat and Mass Transfer Inside a Cone due to a Point Sink. *Journal of Applied Fluid Mechanics*. 4(4), 59-63.
- Carnahan, B., H. A. Luther and J. O. Wilkes (1969). *Applied Numerical Methods*, John Wiley & Sons, New York.
- Carslaw, H. S. and J. C. Jaeger (1959). *Conduction of Heat in Solids*. Oxford Univ. Press, London.
- Chambre, P. L. and J. D. Young (1958). On the diffusion of a chemically reactive species in a laminar boundary layer flow. *The Physics of Fluids*. 1, 48-54.
- Chamkha, A. J. and S. E. Ahmed (2011). Similarity Solution for Unsteady MHD Flow Near a Stagnation Point of a Three-Dimensional Porous Body with Heat and Mass Transfer, Heat Generation/Absorption and Chemical Reaction. *Journal of Applied Fluid Mechanics*. 4(2), 87-94.
- Choudhury, R. and S. Kumar Das (2014). Visco-Elastic MHD Free Convective Flow through Porous Media in Presence of Radiation and Chemical Reaction with Heat and Mass Transfer. *Journal of Applied Fluid Mechanics* 7(4), 603-609.
- Das, U. N., R. K. Deka and V. M. Soundalgekar (1994). Effects of mass transfer on flow past an impulsively started infinite vertical plate with constant heat flux and chemical reaction. *Forschung in Ingenieurwesen* 60, 284-287.
- Das, U. N., R. K. Deka and V. M. Soundalgekar (1999). Effects of mass transfer on flow past an impulsively started infinite vertical plate with chemical reaction. *The Bulletin of GUMA*. 5, 13-20.
- Das, U. N., R. K. Deka and V. M. Soundalgekar (1999). Transient free convection flow past an infinite vertical plate with periodic temperature variation. *Journal of Heat Transfer* 121, 1091-1094.
- Emerly-Ashly, F. (1963). The effect of magnetic field upon the free convection of a conducting fluid. *Journal of Heat Transfer* 85(2), 119-124.
- Ganesan, P. and H. P. Rani (1998). Transient natural convection along vertical cylinder with heat and mass transfer. *Heat and Mass transfer* 33, 449-455.
- Ganesan, P. and P. Loganathan (2001). Unsteady free convection flow over a moving vertical cylinder with heat and mass transfer. *Heat and Mass Transfer* 37(1), 59-65.
- Hossain, M. A. (1988). Simultaneous heat and mass transfer on oscillatory free convection boundary layer flow. *International Journal of Energy Research* 12, 205-206.
- Kao, T. T. (1976). Locally non-similar solution for laminar free convection adjacent to a vertical wall. *Journal of Heat Transfer* 98, 321-322.
- Kishore, P. M., V. Rajesh and S. V. K. Varma (2010). The effects of thermal radiation and viscous dissipation on MHD heat and mass diffusion flow past a surface embedded in a porous medium. *Int. J. of Appl. Math and Mech*. 6(11), 79-97.
- Kumari, M. and G. Nath (1999). Development of two-dimensional boundary layer with an applied magnetic field due to impulsive motion. *Indian Journal of Pure and Applied Mathematics* 30(7), 695-708.
- Li, J., D. B. Ingham and I. Pop (2001). Natural convection from a vertical plate with a surface temperature oscillation. *International Journal of Heat and Mass Transfer* 44, 2311-2322.
- Loganathan, P., M. Kannan and P. Ganesan (2011). MHD effects on free convection flow over a moving semi-infinite vertical cylinder with temperature oscillation. *Appl. Math. Mech. – Engl. Ed.* 32(11), 1367-1376.
- Muthucumaraswamy, R. and P. Ganesan (2000). On impulsive motion of a vertical plate with heat flux and diffusion of chemically reactive species. *Forschung im Ingenieurwesen*. 66, 17-23.
- Na, T. Y. (1978). Numerical solution of natural convection flow past a non-isothermal vertical flat plate. *Applied Scientific Research* 33, 519-

543. *Journal of Energy Heat and Mass Transfer* 19, 273–278.
- Rajesh, V. (2012). Effects of mass transfer on flow past an impulsively started infinite vertical Plate with newtonian heating and chemical Reaction. *Journal of Engineering Physics and Thermophysics* 85, 1:221-228.
- Rajesh, V., A. J. Chamkha, D. Bhanumathi and S. Vijaya kumar varma (2013). Radiation and chemical reaction effects on unsteady MHD free convection flow of a dissipative fluid past an infinite vertical Plate with newtonian heating. *Computational Thermal Sciences* 5 (5), 355-367.
- Rees, D. A. S. (1997). Three-dimensional free convection boundary layers in porous media induced by a heated surface with spanwise temperature variations. *Journal of Heat Transfer* 119, 792-798.
- Saeid, N. H. (2004). Periodic free convection from vertical plate subjected to periodic surface temperature oscillation. *International Journal of Thermal Sciences* 43, 569-574.
- Schlichting, H. (1979). *Boundary Layer Theory*. New York, McGraw-Hill.
- Shankar, B. and N. Krishan (1997). The effect of mass transfer on the MHD flow past an impulsively started infinite vertical plate with variable temperature or constant heat flux.
- Soundalgekar, V. M., R. M. Lahurikar, S. G. Pohanerkar, and N. S. Birajdar (1994). Effects of mass transfer on the flow past an oscillating infinite vertical plate with constant heat flux. *Journal of Thermophysics and Aeromechanics* 1, 119-124.
- Soundalgekar, V. M., S. G. Pohanerkar and N. S. Birajdar (1995). Mass transfer effects on flow past a vertical oscillating plate with variable temperature. *Heat and Mass Transfer* 30(5), 309-312.
- Uddin, M. S., K. Bhattacharyya, G. C. Layek and W.A. Pk (2011). Chemically Reactive Solute Distribution in a Steady MHD Boundary Layer Flow over a Stretching Surface. *Journal of Applied Fluid Mechanics* 4(4), 53-58.
- Yang, J., D. R. Jeng and K. J. DeWitt (1982). Laminar free convection from a vertical plate with non-uniform surface conditions. *Numerical Heat Transfer* 5, 165-184.
- Zhang, X. R., S. Maruyama and S.Sakai (2004). Numerical investigation of laminar natural convection on a heated vertical plate subjected to a periodic oscillation. *International Journal of Heat and Mass Transfer* 47, 4439-4448.